

Polymer Chemistry

Volume 16
Number 9
7 March 2025
Pages 1013-1112

rsc.li/polymers



ISSN 1759-9962



ROYAL SOCIETY
OF CHEMISTRY

COMMUNICATION

Bert Klumperman *et al.*
Bioderived copolymer alternatives to poly(styrene-co-maleic anhydride) *via* RAFT-mediated copolymerization

15
YEARS
ANNIVERSARY

Cite this: *Polym. Chem.*, 2025, **16**, 1019Received 31st October 2024,
Accepted 7th January 2025

DOI: 10.1039/d4py01227e

rsc.li/polymers

Bioderived copolymer alternatives to poly(styrene-co-maleic anhydride) via RAFT-mediated copolymerization†

Lauren Elaine Ball,  ‡ Michael-Phillip Smith  ‡ and Bert Klumperman  *

Poly(styrene-co-maleic anhydride) (SMANh) is a petroleum-based copolymer with desirable properties that afford utility in both industrial and academic fields. The reversible addition–fragmentation chain transfer (RAFT)-mediated polymerization of the bioderived comonomers, indene and itaconic anhydride, was explored using three chain transfer agents with varying activity, and generally well-controlled ($\bar{D} < 1.40$) polymerizations were observed.

Poly(styrene-co-maleic anhydride) (SMANh) is synthesized *via* the copolymerization of the petroleum-derived comonomers, styrene (STY) and maleic anhydride (MANh) and is readily hydrolysed in alkaline media yielding the amphiphilic copolymer, poly(styrene-co-maleic acid) (SMA). SMA has been employed in a variety of biomedical applications such as drug delivery,^{1–3} lipid nanodisc formation and membrane protein isolation,^{4–6} and hydrogel formation.^{7,8} The copolymerization of STY and MANh is well-established,⁹ with ongoing improvements realized through the application of controlled polymerization methodologies *e.g.* RAFT-mediated polymerization. The synthesis of SMANh *via* RAFT-mediated polymerization affords desirable properties such as targeted molecular weights, low \bar{D} and functional chain ends which provide access to various polymer architectures.^{4–6,10}

The increasing need for the development of “greener” synthetic protocols and “green” polymer alternatives can be assuaged through the careful selection of monomers which are bioderived instead of petroleum-derived. The selection of appropriate bioderived monomers, similar in structure to their petroleum-based counterparts, needs to be undertaken with care to retain the targeted chemical composition and physical properties of the copolymer. Ideally suited and poorly explored greener alternatives to STY and MANh are indene (Ind),^{11–14}

and itaconic anhydride (IANh),^{15,16} respectively. These monomers are derived from renewable feedstocks and differ chemically by a single CH₂ group from their petroleum-based counterparts. Despite the slight difference in chemical structure, it is hypothesized that well-defined “greener” copolymers with similar properties and biomedical relevance comparable to SMANh can be synthesized. To the best of our knowledge, there is negligible data available for the RAFT-mediated synthesis of poly(styrene-*alt*-itaconic anhydride) (SIAnh), poly(indene-*alt*-itaconic anhydride) (IIAnh), and poly(indene-*alt*-maleic anhydride) (IMAnh), where these systems have only been investigated *via* conventional radical polymerizations,^{17–19} or single-unit monomer insertion (SUMI) reactions.^{20–23} The investigation presented here provides insight into the unexplored RAFT-mediated copolymerization of these bioderived comonomers, towards the synthesis of well-defined SIAnh, IIAnh, and IMAnh copolymers as SMANh alternatives. For each SMANh alternative, systematic replacement of one or both comonomers in the copolymerization reaction was undertaken (summarized in Fig. 1). A representative CTA from each “CTA class” was selected, including a dithiobenzoate (CTA1),^{5,24–27} trithiocarbonate (CTA3),^{4,6,28} and universal-type dithiocarbamate (CTA2),²⁹ where the two former classes are commonly used CTAs for SMANh copolymerizations and the latter CTA has recently been successfully employed for the synthesis of SMANh and its analogues (Ball *et al.* – manuscript in preparation). Xanthates were excluded from kinetic experiments in this study, as they do not provide adequate control over the four RAFT-mediated copolymerizations investigated (Table S1†).³⁰

As a basis of comparison, styrene and maleic anhydride were copolymerized to afford SMANh using two commonly used RAFT agents (CTA1 and 3),^{4,5} and a universal RAFT agent (CTA2) not typically employed for SMANh copolymerizations (Table 1). For all SMANh copolymerizations, M_n increased linearly with increasing monomer conversion (α) and low dispersities were observed for SMANh1 and SMANh2 throughout the copolymerization, with a decrease in \bar{D} with increasing α

Department of Chemistry and Polymer Science, Stellenbosch University, Matieland
7602, South Africa. E-mail: bklump@sun.ac.za

† Electronic supplementary information (ESI) available. See DOI: <https://doi.org/10.1039/d4py01227e>

‡ Both authors contributed equally to this work.



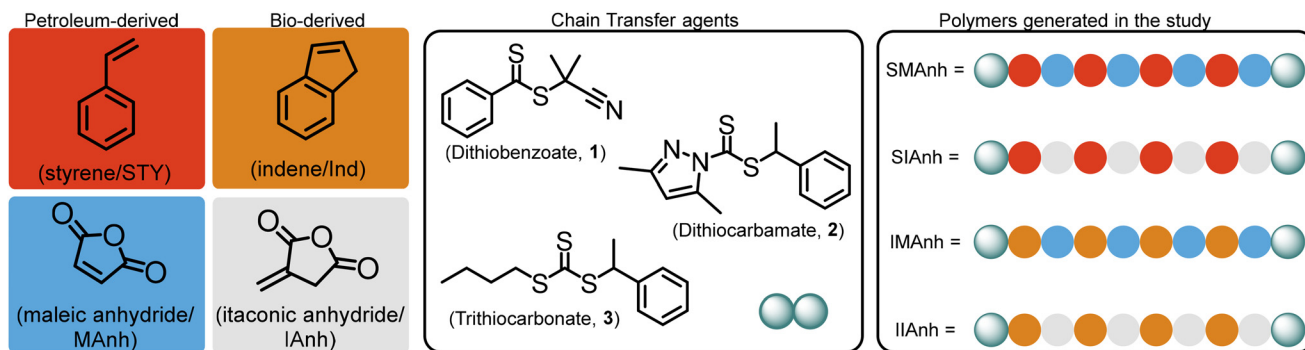


Fig. 1 Copolymers synthesized using styrene (STY), indene (Ind), maleic anhydride (MAAnh), and itaconic anhydride (IAAnh). poly(styrene-*alt*-maleic anhydride) (SMAAnh), poly(styrene-*alt*-itaconic anhydride) (SIAnh), poly(indene-*alt*-itaconic anhydride) (IIAnh), poly(indene-*alt*-maleic anhydride) (IMAnh).

Table 1 Summary of RAFT-mediated copolymerizations conducted in 1,4-dioxane at 70 °C with a CTA : AIBN of 1 : 0.2 (additional experimental data available in the ESI†). The recommended RAFT system for each comonomer pair is indicated by a highlighted row. All copolymers were characterized via SEC, ¹H NMR and ATR-FTIR spectroscopy (Fig. S7–13†)

Copolymer ^a	α 24 h ^b (%)	M_n^{theo} ^c (g mol ⁻¹)	M_n^{SEC} ^d (g mol ⁻¹)	D^d
SMAAnh1	93	9700	9200	1.18
SMAAnh2	98	10 000	10 200	1.13
SMAAnh3	93	10 100	9500	1.17
IMAnh1	51	5300	3600	1.26
IMAnh2	97	9900	6100	1.37
IMAnh3	98	9100	6200	1.25
SIAnh1	STY – 93; IAAnh – 97	10 400	8000	1.15
SIAnh2	STY – 93; IAAnh – 97	10 600	7700	1.25
SIAnh3	STY – 39; IAAnh – 79	6700	4500	1.37
IIAnh1	Ind – 20; IAAnh – 45	3800	3400	1.29
IIAnh2	Ind – 47; IAAnh – 74	6900	3100	1.64
IIAnh3	Ind – 57; IAAnh – 83	7900	3600	1.55

^a Copolymer legend provided in Fig. 1, where the number in bold refer to the CTA utilized. ^b Monomer conversion determined via ¹H NMR spectroscopy using 1,3,5-trioxane as internal reference and eqn (S1).† ^c Calculated using eqn (S2).† ^d Determined via SEC analysis using THF (5% AcOH) as mobile phase and PS calibration standards.

observed for SMAAnh3 & 2 (Fig. 2, Fig. S1†). The strong correlation between M_n^{theo} and M_n^{SEC} would suggest all CTA was converted to macro-CTA. CTA1 appears to retard the RAFT-mediated copolymerization of STY and MAAnh significantly, where the k_p^{app} of the SMAAnh2 and SMAAnh3 copolymerization were higher than that observed for SMAAnh1 (Table S1†). Furthermore, an initialization period (~1 h) was observed for SMAAnh1, during which only ~2% comonomer conversion was obtained (Fig. S1†). This behaviour is well-known for dithiobenzoates and has been demonstrated for the RAFT-mediated synthesis of SMAAnh previously.²⁴ The reactivity ratios for this comonomer system, and others investigated in this study, were determined (Table 2) and are further discussed in Table S2.† Similar RAFT-mediated copolymerizations (using CTA1, 2 and 3) were investigated, with the replacement of the STY comonomer with Ind, to afford IMAnh. Unsurprisingly, all copolymerizations displayed a strong alternating character,³¹ where CTA2

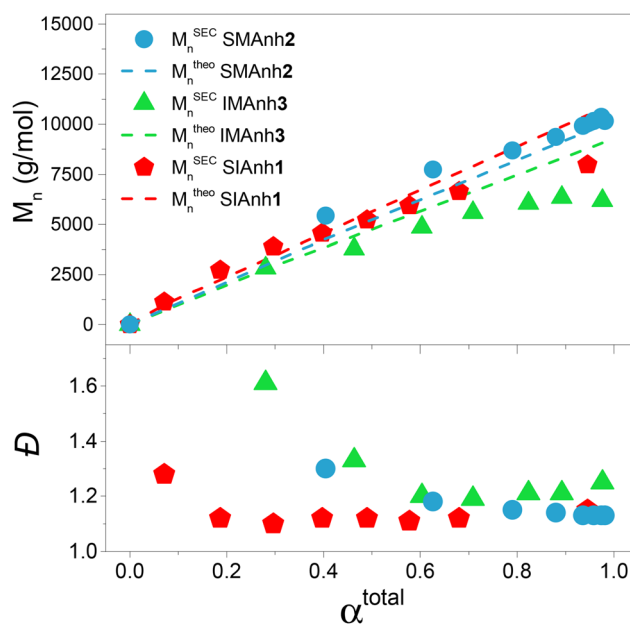


Fig. 2 Evolution of M_n^{SEC} and D with increasing monomer conversion for well-controlled SMAAnh, SIAnh and IMAnh copolymerizations.

Table 2 Reactivity ratios of the respective comonomer systems mediated with CTA3

	STY (r_1)	Ind (r_1)
MAAnh (r_2)	$r_1 = 0.01$; $r_2 = 0.01$	$r_1 = 0.01$; $r_2 = 0.01$
IAAnh (r_2)	$r_1 = 0.12$; $r_2 = 0.01$	$r_1 = 0.01$; $r_2 = 0.13$

and 3 were determined to be most suitable for the synthesis of well-defined IMAnh in good yield. IMAnh1 and IMAnh3 exhibited a generally linear evolution of M_n and decreasing D with increasing α , suggesting the copolymerization was well-controlled (Fig. 2, and Fig. S2†). Slower polymerization kinetics were observed for all instances of IMAnh (1–3) copolymerization compared to the respective SMAAnh systems (Fig. S2, and Table S1†), potentially due to the increased substitution from



a monosubstituted monomer (STY) to a 1,2-disubstituted monomer (Ind), resulting in a more stabilized vinyl bond. A computational analysis of a model IMAnh copolymerization showed that the Gibbs free energy required for a MAnh-based radical to react with Ind is less favourable compared to STY ($\Delta G_{\text{STY, addition}} = -5.6 \text{ kcal mol}^{-1}$ and $\Delta G_{\text{Ind, addition}} = -1.5 \text{ kcal mol}^{-1}$, Fig. S21 & S23†). This is further supported by the higher LUMO energy of Ind ($-0.03 \text{ Hartree} = \text{double bond}$) compared to STY ($-0.05 \text{ Hartree} = \text{double bond}$) (Fig. S20†).

CTA1 caused significant retardation of the IMAnh copolymerization kinetics (in addition to retardation derived from Ind), with a longer initialization period ($\sim 2 \text{ h}$) observed compared to the SMAnh1 copolymerization (Fig. S2†). As a result, low monomer conversion was obtained (50% within 24 h). Despite this, IMAnh1 copolymers with low D and good correlation between M_n^{theo} and M_n^{SEC} were obtained. For all IMAnh copolymerizations, a deviation of M_n^{SEC} from M_n^{theo} was observed at higher monomer conversions, accompanied by an increase in D (Fig. S2†). $^1\text{H NMR}$ spectroscopic analysis of IMAnh copolymerization kinetic samples showed full consumption of CTA1 within 3 h and CTA2/CTA3 within 1 h, which would suggest reasonable Z- and R-group efficiencies. Therefore, the deviation of M_n^{SEC} at high α is tentatively attributed to inefficient reinitiation of the macro-CTA leaving group, as SEC analysis revealed low molecular weight tailing in the RI eluogram which was also present in the corresponding UV eluogram (320 nm) (Fig. S12†). SMAnh and IMAnh have a strong alternating character as a result of the inability of MAnh to homopolymerize. Contrarily, the homopolymerization of IAnh has been reported in literature.⁹ SIAnh copolymerizations generally exhibited slower kinetics compared to the corresponding SMAnh copolymerizations, with only slightly higher rates of IAnh consumption compared to STY observed for SIAnh1 and SIAnh2 (Fig. S3†). Inspection of the copolymerization kinetics for SMAnh1 and SIAnh1 shows that similar k_p^{APP} values are obtained. This result is interesting as it indicates that the substitution pattern of the double bond of IAnh does not impact the rate of polymerization significantly (1,1 vs. 1,2 disubstituted monomers). CTA1 was fully converted to macro-CTA within 1 h (Fig. S5†) without the presence of a prominent initialization period, where M_n^{SEC} evolved linearly with increasing α and low D was maintained throughout the copolymerization (Fig. 2). CTA2 and CTA3 were converted to macro-CTA slowly throughout the copolymerization, where 12% and 7% of CTA2 and CTA3 remained at 24 h, respectively (Fig. S5 and 6†). The RAFT pre-equilibrium for SIAnh3 and SMAnh3 was assessed computationally (Fig. S16 and 17†), where the former exhibited significantly slower consumption of CTA3 than the latter. The addition of IAnh to CTA3 to form the corresponding intermediate radical was energetically unfavourable compared to the addition of MAnh ($\Delta G_{\text{MAnh, addition}} = 13.7 \text{ kcal mol}^{-1}$ vs. $\Delta G_{\text{IAnh, addition}} = 24.7 \text{ kcal mol}^{-1}$). Furthermore, the fragmentation of the MAnh-based intermediate radical favoured the generation of R-group re-initiating radicals (promoting an efficient pre-equilibrium), whereas the fragmentation of IAnh-based intermediate radicals favoured the regeneration of IAnh-based radicals

(resulting in an inefficient pre-equilibrium) (Fig. S16 and 17†). SEC analysis of SIAnh2 and SIAnh3 showed low molecular weight tailing in the RI eluograms which had an associated UV signal (320 nm), which in this case likely corresponds to the continual formation of low molecular weight SIAnh as CTA2/3 is slowly converted into macro-CTA throughout the copolymerization (Fig. S10 and 11†). While the linear evolution of M_n^{SEC} with increasing α was observed for SIAnh2 and SIAnh3, the inefficient conversion of CTA to macro-CTA resulted in poor correlation between M_n^{SEC} and M_n^{theo} and relatively high D throughout the copolymerization (Fig. S3†).

Lastly, attempts were made to copolymerize the fully bioderived comonomer pair (Ind and IAnh) *via* RAFT-mediated copolymerization. None of the CTAs investigated could provide an adequate level of control over the RAFT-mediated copolymerization of Ind and IAnh (Fig. S4†). Inspection of the kinetic samples *via* $^1\text{H NMR}$ spectroscopy showed that **CTA1** was fully converted to macro-CTA within 3 h, while **CTA2** and **CTA3** were consumed slowly throughout the copolymerization, with a total consumption of 79% and 95%, respectively (Fig. S5 and 6†). The IAnh3 RAFT pre-equilibrium, and the propagation of Ind- and IAnh-based radicals, were assessed computationally (Fig. S19 & S24,† respectively). Overall, the differences in reactivity of the Ind- and IAnh-based propagating radicals suggest that during the main equilibrium, intermediate radicals predominantly constitute IAnh terminal leaving groups. During the RAFT pre-equilibrium, the fragmentation of the IAnh-based intermediate radical favours the generation of IAnh-based propagating radicals as opposed to R-group re-initiating radicals (critical analysis of the IAnh RAFT-mediated copolymerization available in the ESI†). Thus, it is plausible that IAnh is a better polymeric leaving group compared to the 1-phenyl ethyl R-group, resulting in slow consumption of CTA2 and CTA3 throughout the copolymerization. Inspection of the RI eluograms for IAnh3 shows that a shift towards lower elution volumes with copolymerization time can be observed, but due to the inefficient consumption of the CTA throughout the copolymerization, the M_n remains relatively constant with increasing monomer conversion (Fig. S13†) and consequently, high D (>1.5) was observed throughout the copolymerization. The kinetic analyses of all four comonomer systems, consistently suggest that the itaconic anhydride-containing copolymers have slower polymerization kinetics with inefficient conversion of CTA to macro-CTA. While the RAFT-mediated copolymerization of Ind and IAnh yielded promising results, further critical investigation of the system is required to enable the synthesis of a well-defined, and fully bioderived, copolymer. It is possible that an alternative CTA, with an R-group that is more compatible with the IAnh comonomer, would significantly improve the synthesis of the IAnh-based copolymers.

Conclusions

In this work, the ideal CTAs required for the well-controlled RAFT-mediated copolymerization of petroleum-derived and



bioderived comonomers to afford SMAnh, SIANh, and IMAnh were determined (CTA2, 3 and 1, respectively). The fully bio-derived copolymer IAnh could be synthesized successfully, but IAnh with targeted M_n and low D could not be achieved, due to inefficient conversion of CTA to macro-CTA. Nevertheless, this study has effectively expanded the variety of “greener” SMAnh-type copolymers available for utility in biomedical research. An interrogation of solution properties for these bioderived copolymers and how they compare to SMAnh is currently underway within our research group. The results of this interrogation will provide the tools necessary to tune the chemical composition of the bioderived copolymers such that desirable physical properties are realized.

Author contributions

Lauren Elaine Ball: data curation, formal analysis, investigation, methodology, visualization, writing. Michael-Phillip Smith: conceptualization, computational investigation, data curation, formal analysis, investigation, methodology, project administration, visualization, writing – first draft. Bert Klumperman: supervision, funding acquisition, resources, reviewing and editing.

Data availability

All the data relevant to the current submission has been collated in the ESI.† Raw data, such as NMR, FT-IR and SEC data can be obtained upon request from the authors.

Conflicts of interest

There are no conflicts to declare.

Acknowledgements

We would like to acknowledge and thank the Wellcome Trust (grant no 223728/Z/21/Z), National Research Foundation (NRF, grant no 46855) and Wilhelm Frank Trust for funding this research. The authors further acknowledge the Centre for High-Performance Computing (NICIS CHPC) for access to the computational software that was utilized in this work.

References

- 1 N. Angelova and G. Yordanov, *Colloids Surf., A*, 2014, **452**, 73–81.
- 2 S. Henry, M. El-Sayed, C. Pirie, A. Hoffman and P. Stayton, *Biomacromolecules*, 2006, **7**(8), 2407–2414.
- 3 R. Richard, M. Schwarz, K. Chan, N. Teigen and M. Boden, *J. Biomed. Mater. Res., Part A*, 2009, **90**(2), 522–532.
- 4 R. D. Cunningham, A. H. Kopf, B. O. W. Elenbaas, B. B. P. Staal, R. Pfukwa, J. A. Killian and B. Klumperman, *Biomacromolecules*, 2020, **21**, 3287–3300.
- 5 A. A. A. Smith, H. E. Autzen, T. Laursen, V. Wu, M. Yen, A. Hall, S. D. Hansen, Y. Cheng and T. Xu, *Biomacromolecules*, 2017, **18**, 3706–3713.
- 6 K. M. Burrige, B. D. Harding, I. D. Sahu, M. M. Kearns, R. B. Stowe, M. T. Dolan, R. E. Edelmann, C. Dabney-Smith, R. C. Page, D. Konkolewicz and G. A. Lorigan, *Biomacromolecules*, 2020, **21**, 1274–1284.
- 7 J. Hrib, E. Chylikova Krumbholcova, M. Duskova-Smrckova, R. Hobzova, J. Sirc, M. Hruby, J. Michalek, J. Hodan, P. Lesny and R. Smucler, *Polymers*, 2019, **11**(7), 1087.
- 8 C. Tang, S. Ye and H. Liu, *Polymer*, 2007, **48**, 4482–4491.
- 9 B. Klumperman, *Polym. Chem.*, 2010, **1**, 558–562.
- 10 S. Bag, S. Ghosh, S. Paul, M. E. H. Khan and P. De, *Macromol. Rapid Commun.*, 2021, **42**(23), 2100501.
- 11 E. A. Uslamin, N. Kosinov, G. A. Filonenko, B. Mezari, E. Pidko and E. J. M. Hensen, *ACS Catal.*, 2019, **9**(9), 8547–8554.
- 12 B. Zhang, Z. Zhong, J. Zhang and R. Ruan, *J. Anal. Appl. Pyrolysis*, 2018, **133**, 147–153.
- 13 J. Gancedo, L. Faba and S. Ordóñez, *ACS Sustainable Chem. Eng.*, 2022, **10**(9), 3057–3065.
- 14 S. Li, Y. Li, J. Wu, Z. Wang, F. Wang, L. Deng and K. Nie, *Renewable Energy*, 2020, **155**, 1042–1050.
- 15 M. Okabe, D. Lies, S. Kanamasa and E. Y. Park, *Appl. Microbiol. Biotechnol.*, 2009, **84**, 597–606.
- 16 T. Willke and K. D. Vorlop, *Appl. Microbiol. Biotechnol.*, 2001, **56**, 289–295.
- 17 J. Drougas and R. Guile, *J. Polym. Sci.*, 1961, **55**(6), 161.
- 18 D. Tohru and M. Yuji, *Macromolecules*, 1978, **11**(1), 270–274.
- 19 L. F. Kim, L. L. Stotskaya, B. A. Krentsel, V. P. Zubov, V. B. Golubev and I. L. Stoyachenko, *J. Macromol. Sci., Part A: Pure Appl. Chem.*, 1978, **12**, 1197–1210.
- 20 K. Hakobyan, B. Noble and J. Xu, *Chem. Commun.*, 2024, **60**, 7443–7446.
- 21 K. Hakobyan, B. B. Noble and J. Xu, *Polym. Chem.*, 2023, **14**, 4116–4125.
- 22 Z. Huang, B. B. Noble, N. Corrigan, Y. Chu, K. Satoh, D. S. Thomas, C. J. Hawker, G. Moad, M. Kamigaito, M. L. Coote, C. Boyer and J. Xu, *J. Am. Chem. Soc.*, 2018, **140**, 13392–13406.
- 23 R. Liu, L. Zhang, Z. Huang and J. Xu, *Polym. Chem.*, 2020, **11**, 4557–4567.
- 24 E. T. A. van den Dungen, J. Rinqest, N. O. Pretorius, J. M. McKenzie, J. B. McLeary, R. D. Sanderson and B. Klumperman, *Aust. J. Chem.*, 2006, **59**, 742–784.
- 25 S. Sirohi, M. Jassal and A. K. Agrawal, *Appl. Nanosci.*, 2018, **8**, 1701–1710.
- 26 M. C. Davies, J. V. Dawkins and D. J. Hourston, *Polymer*, 2005, **46**(6), 1739–1753.
- 27 H. De Brouwer, M. A. J. Schellekens, B. Klumperman, M. J. Monteiro and A. L. German, *J. Polym. Sci., Part A: Polym. Chem.*, 2000, **19**(38), 3596–3603.



- 28 J. Ma, C. Cheng, G. Sun and K. L. Wooley, *Macromolecules*, 2008, **41**(23), 9080–9089.
- 29 J. Gardiner, I. Martinez-Botella, J. Tsanaktsidis and G. Moad, *Polym. Chem.*, 2016, **7**, 481–492.
- 30 D. J. Keddie, G. Moad, E. Rizzardo and S. H. Thang, *Macromolecules*, 2012, **45**(13), 5321–5342.
- 31 T. Doiuchi and Y. Minoura, *Macromolecules*, 1978, **11**(1), 270–274.

